Environ Geochem Health (2020) 42:3119–3130
https://doi.org/10.1007/s10653-020-00546-x

ORIGINAL PAPER

Temporal and spatial assessment of groundwater contamination with nitrate by nitrate pollution index (NPI) and GIS (case study: Fasarud Plain, southern Iran)

Mehdi Bahrami · Abdol Rassoul Zarei · Farideh Rostami

Received: 22 August 2019 / Accepted: 28 February 2020 / Published online: 7 March 2020

Abstract Groundwater resources in arid and semi-arid regions are the most and sometimes the only water resource used for agricultural, industrial, and urban water supply. Irregular and immense application of nitrogen fertilizers in the lands under cultivation and nitrate leakage from livestock farming have affected the groundwater quality. In such areas, nitrate is one of the main pollutants in the groundwater. In this study, the temporal and spatial trend of nitrate contamination in 31 wells in Fasarud Plain, southern Iran, from April 2017 to March 2018 were assessed. To survey the geochemical quality of the plain, a geographic information system to expand geographic location maps and spatial distribution maps of nitrate concentration and nitrate pollution index (NPI) was applied. Nitrate concentrations ranged between 2.43 and 96 mg L^{-1}. Results indicated that nitrate temporal trend was increased significantly in most of the wells, and the spatial trend of area percentage of nitrate class 3 (not permissible limit of more than 50 mg L^{-1}) was positive. The greatest quantities of this variable in groundwater samples detected in northern, western, and eastern areas of the plain have a direct relation with the fertilization of agricultural lands. Generally, by ending the irrigation season, nitrate concentration and NPI reduced temporally in the samples and the percentage area of nitrate class 3 decreased gradually, again beginning the agricultural season, the NPI, nitrate concentration, and percentage area of nitrate class 3 began to increase. Overall, the change of nitrate concentration and distribution of agricultural regions have illustrated that nitrate originated from nitrogenous inorganic fertilizers applied within irrigation periods.

Keywords Nitrate · Groundwater · Water contamination · GIS · NPI

Introduction

The rapid population growth, urbanization, industrialization, and the rise of living standards have contributed to environmental pollution, especially in drinking water supplies (Zarei and Bahrami 2016; Mokarram et al. 2015b, c; Naseri et al. 2006). The development process in Iran has caused many

M. Bahrami (✉)
Department of Water Engineering, Faculty of Agriculture, Fasa University, Fasa, Iran
e-mail: bahrami@fasau.ac.ir

A. R. Zarei
Department of Range and Watershed Management (Nature Engineering), Faculty of Agriculture, Fasa University, Fasa, Iran
e-mail: Ar_Zareiee@Fasau.ac.ir

F. Rostami
Department of Water Engineering, Faculty of Agriculture, Fasa University, Fasa, Iran
e-mail: frstmi343@gmail.com

problems including water pollution; this issue becomes more important since Iran is placed in an arid and semi-arid area and groundwater supplies about 52% of drinking water (Mokarram et al. 2015c; Beiranvand et al. 2014). Regarding the lack of water and drought crises in recent years, the importance of groundwater has been increasing day by day mainly in the western United States (Turner et al. 2019) and Asian countries such as Iran (Nosrati and Zareiee 2011; Bahrami et al. 2017, 2018; Abou Zaki et al. 2019), India (Voss et al. 2013; Mukherjee et al. 2018), Bangladesh (Mojid et al. 2019), China (Werner et al. 2013), and Saudi Arabia (Michel et al. 2012).

The greatest threat to the groundwater in the future is the pollution of this source by harmful substances entered by humans deliberately or unintentionally or as a result of negligence and ignorance. Nitrate is the most abundant and perhaps the most common pollutant that threatens groundwater. Nitrate is the most prevalent groundwater contaminant detected specifically in shallow aquifers because of both point and nonpoint sources (Esmaeili et al. 2014). This ion in drinking water has two undesirable health effects including methemoglobinemia or "blue baby" syndrome in infants and the potential of carcinogenic compounds in adults (Schipper and Vojvodić-Vuković 2000). Liu et al. (2017) assessed the concentration and spatiotemporal distribution of groundwater nitrate under cropland by statistical and geostatistical techniques in Shandong province, China. Results revealed that the median nitrate concentrations after the rainy season were considerably more than those before the rainy season, and reduced with enhancing groundwater depth. Also, nitrate under the vegetable and orchard area is considerably more than the ones under grain. The kriging map indicated that groundwater nitrate has a powerful spatial variation.

During the past two centuries, production and consumption of nitrate, especially in the agricultural field, have been increased considerably. Currently, many countries in the world including Iran (Badee Nezhad et al. 2017), India (Devendra et al. 2016), China (Meng et al. 2018), etc., encounter a high nitrate level in drinking water. The main reason is the recharge of agricultural runoff and municipal and industrial wastewater to water resources, particularly groundwater. Ducci (2018) presented a technique for evaluating nitrate pollution susceptibility in groundwater applying thematic maps. The results of this paper showed a partly good correlation coefficient between the created nitrate pollution susceptibility map and the nitrate distribution in groundwater in the study area. Han et al. (2018) assessed the sources and processing of nonpoint sources of nitrate in China. The results of the spatial analysis indicated that NO_3 concentration was great in the tea plantation and forest zones, and in the temporal analysis showed a high NO_3 level in spring.

Green et al. (2018) assessed the zonal variation of nitrate fluxes in the unsaturated zone and groundwater in Wisconsin. Results indicated that under common activities and conditions, almost 60% of the shallow aquifer will finally be impressed by the downward migration of NO_3^-, with denitrification protecting the remaining 40%. Akpan et al. (2018) evaluated the spatial distribution of pollutants and their values in soil and water resources applying geophysical and geological data include pH, EC, TDS, Cl^-, NO_3^-, HCO_3^-, HCO_3^-, SO_4^{2-}, Ca^{2+}, Na^+, K^+ and Mg^{2+} in Nigeria. The findings indicated that ionic concentrations in the sand-dominated soils and water were within permissible limits and baseline standards.

In recent years, numerous studies have been conducted to investigate the nitrate pollution in the water resources (Chand et al. 2011; Maghanga et al. 2013; Ameur et al. 2016; Hoseinzadeh et al. 2016; Akale et al. 2018; Sun and Chai 2018; Jahangeer Gupta and Yadav 2018; Ducci et al. 2019; Mir et al. 2019; Ogrinc et al. 2019; Rawat et al. 2019; Yin et al. 2019). Based on the conclusion of researches done in Iran, nitrate contamination in the water resources of Iran is at a medium level. In most of the researches, high nitrate concentrations are because of lack of sewage collection networks, discharge of urban and industrial sewage to water resources, and agricultural practices that apply high values of manure and fertilizer (Akhavan et al. 2014). Therefore, the present study is aimed to assess the temporal and spatial trend of nitrate contamination in Fasarud Plain groundwater, southern Iran, using GIS and demonstrate the achieved findings by using nitrate pollution index (NPI).

Materials and methods

This study utilized groundwater quality data collected from 31 water wells of Fasarud Plain, Darab County, Iran, from April 2017 to March 2018 (in total, 279 samples). In each well, the samples were taken after a pumping period of 10 min at least. The water samples were collected in polyethylene bottles. They were stored in the refrigerator until they were analyzed (Mousavi and Amiri 2012). The nitrate concentration was measured by spectrophotometry method (APH 1998; Wang et al. 1998). For this, an aliquot (50 mL) of water sample was transferred to a 100 ml beaker, 1 mL HCl (1.0 N) was added. The absorbance of the sample was measured at 220 nm (NO_3 + organic matter) by spectrophotometer. Then, the absorbance of the sample was measured at 275 nm (organic matter). If Abs275 nm × 2 < 10% Abs220 nm, the Abs275 nm × 2 was subtracted from Abs220 nm to obtain value for NO_3 corrected for organic matter content.

Validation of chemical analysis results was performed by the ionic balance verification and by repeating the analysis for the same sample. The precision of the results was estimated by calculating the charge balance error (CBE). The test results are considered reliable only when the CBE is less than or equal to 5% (Guangwei, 2013). The limit of nitrate content in drinking water has set by the World Health Organization (WHO 2011) and also the Institute of Standards and Industrial Research of Iran (ISIRI, 2009) at 50 mg L^{-1}. Based on the achieved findings for the nitrate concentration, water quality was classified into three classes as Table 1.

Then, nitrate contamination of the studied area was assessed by the nitrate pollution index (NPI). To evaluate the nitrate changes over the district within a year, spatial and temporal trends analysis were employed.

Study area

The Fasarud Plain is placed in the Fars Province (the south part of Iran) and extends geographically between 54° 13′ and 54° 32′ East longitude and from 28° 39′ to 28° 49′ North latitude (Fig. 1). The total area of the studied region is 7500 km^2 with an altitude of 1180 m. According to the De Martonne index, the climate of Fasarud Plain is semi-arid, the mean annual temperature is about 25 degrees Celsius, the mean annual rainfall is 350 mm, the mean annual wind speed is about 1.2 m s^{-1}, the mean annual potential evapotranspiration is about 1821.1 mm, and the mean annual sunshine is about 9.4 h day^{-1}.

According to Fig. 1, the most area of the Fasarud Plain is composed of alluvial formation that resulted in the agricultural occupations using groundwater resources as irrigation water supply. The Korsia salt diapir (Sp) is specified in the north of plain. Throughout the north plain including around the salt diapir is formed almost exclusively by Tarbur limestone (Tb), which is a predominantly carbonate lithostratigraphic unit that outcrops in Zagros basin (Maghfouri-Moghadam et al. 2009). The Asmari limestone (As) formation is represented in east and south of plain, that is of Late Oligocene (Chattian) Early Miocene (Burdigalian) age and the youngest source rock in Zagros (Maghfouri-Moghadam and Khanjani 2014). The Upper Cretaceous–Paleocene Gurpi Formation (Cpm) consists of deep-marine shales, marls, and argillaceous lime mudstones that crop out in the Zagros Mountains (Beiranvand et al. 2014), is represented in west and northwest of Fasarud Plain.

Nitrate pollution index

A single-parameter water quality index named the nitrate pollution index (NPI) was applied for

Table 1 Values and categories of NPI and WHO limits on NO_3 (WHO 2011; Almasi et al. 2016; Obeidat et al. 2012)

NPI value	NPI interpretation	NPI class	NO_3 (mg L^{-1})	WHO standard	NO_3 Class
< 0	Clean (unpolluted)	1	< 50	Desirable limit (DL)	1
0–1	Light pollution	2	= 50	Maximum permissible limit (MPL)	2
1–2	Moderate pollution	3	> 50	Not permissible limit (NPL)	3
2–3	Significant pollution	4			
> 3	Very significant pollution	5			

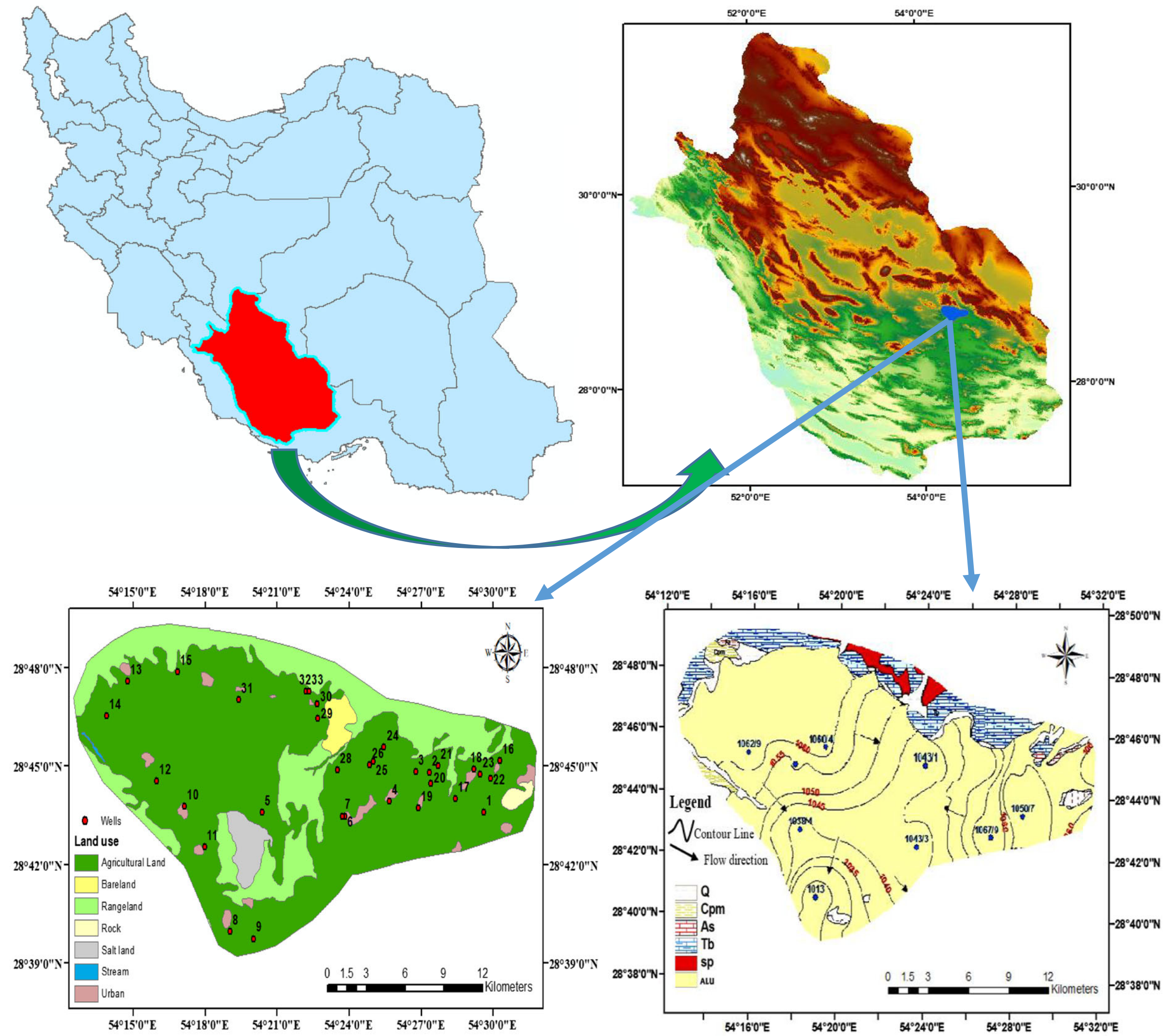

Fig. 1 Land use map and groundwater flow direction of studied area with spatial distribution of the studied wells

measurement of the nitrate pollution in the investigated wells. Applying the NPI index is indicative of nitrate pollution in the groundwater due to anthropogenic activity. The following formula was applied to compute the NPI (Obeidat et al. 2012):

$$\mathrm{NPI} = \frac{C_s - \mathrm{HAV}}{\mathrm{HAV}} \quad (1)$$

where C_s is the nitrate concentration in the sample, and HAV is the threshold value of the anthropogenic source (human-affected value), taken as 20 mg L^{-1} (Obeidat et al. 2012). According to the achieved findings for the NPI, water quality was classified into five categories as Table 1.

Temporal trend analysis

Plenty of statistical methods (parametric or nonparametric) have been developed to find trends within time series such as linear regression, Spearman's Rho test, Mann–Kendall test, Sen's slope estimator, and Bayesian method. In the present research, after assessing the normality of nitrate data series by Shapiro-Wilk method (the variables of normality tests were the stations), the trend of these series was evaluated based on the Pearson method (parametric method) and the Spearman's Rho test (nonparametric method), for normal and non-normal values of nitrate, respectively.

Pearson test

Pearson *r* correlation is the most extensively applied correlation statistic to estimate the degree of the relationship between linearly related parameters. Pearson *r* correlation is applied to calculate the degree of relationship between the two parameters. The following formula is applied to measure the Pearson *r* correlation:

$$r = \frac{N\sum xy - (\sum x)(\sum y)}{\sqrt{\left[N\sum x^2 - (\sum x)^2\right]\left[N\sum y^2 - (\sum y)^2\right]}} \quad (2)$$

where N is the number of observations, X is the independent variable, Y is dependent variable, and r is correlation between X and Y.

Spearman's Rho test

Spearman's Rho test is a nonparametric technique customarily applied to verify the absence of tendencies. This test is a statistical measure of the strength of a monotonic relationship between paired data. At Spearman's Rho test, the positive quantities of correlation coefficient show the upward trend in data series and the negative quantities of correlation coefficient show the downward trend in data series. In this test, statistic D is represented as follows (Sneyers 1990):

$$D = 1 - \frac{6\sum_{i=1}^{n}(R(X_i) - i)^2}{n(n^2 - 1)} \quad (3)$$

where $R(X_i)$ is the rank of the observation, X_i is in the time series and, n is the length of the time series.

Spatial trend analysis

There are many interpolation methods for the analysis of the spatial distribution of different parameters, such as geostatistical analysis including inverse distance weighting (IDW), Kriging, and Co-Kriging with Circular, Gaussian, Spherical, and many other variograms (Nazaripur et al. 2015). In the current study, after assessing the nitrate data normality using the Shapiro-Wilk method (using SPSS Software), ArcGIS10.2 interpolation techniques were used to prepare nitrate spatial distribution maps in the studied area (from April 2017 to March 2018 on a monthly basis). Hence, inverse distance weighting (IDW) geostatistical wizard (with pixel size equal to 10 × 10 m) was used to interpolate the data series of nitrate that was non-normal (sig. < 0.05), but for those series of data that was normal, various geostatistical wizards were tested to find the appropriate interpolation method. In this regard, the error criterion of root means square error (RMSE) was used to assess the accuracy and precision of various interpolation methods. Finally, area percentages of each three nitrate classes were extracted from the prepared spatial maps.

After the preparation of nitrate maps and calculation of area percentages for each nitrate class, the normality of data series of area percentages over time was assessed using Shapiro-Wilk's statistical test. Then, the trend of the change of area percentages of different nitrate classes over time (monthly scale) was assessed based on statistical parametric (Pearson) and nonparametric (Spearman's Rho) tests, for normal and non-normal values of data, respectively.

Results and discussion

The statistics of NO_3 and NPI parameters based on all wells are represented in Table 2. The minimum value of nitrate concentration was observed at Well 22 located at the east of plain in June (2.43 mg L^{-1}) and maximum value allocated to Well 16 located in the same area in March (96 mg L^{-1}). The minimum value of NPI was observed at Well 22 in June (− 0.88) while the maximum value allocated to Well 12 in the northwest in September (3.80). Based on the agricultural use of the lands around these wells, the maximum values of nitrate concentration and NPI were observed in months that irrigation was practiced and the minimum quantities were in the months that irrigation

Table 2 Descriptive analysis of nitrate (mg L^{-1}) and NPI in the studied wells

Parameter	Min	Max	Mean	SD	CV
NO_3 (mg L^{-1})	2.43	96	41.32	26.56	0.64
NPI	− 0.88	3.80	1.07	1.33	1.24

CV coefficient variation, *SD* standard deviation had been stopped. Also, according to the mean value of NO_3 concentration equal 41.32 mg L^{-1} and the mean value of NPI equal 1.07, it can be concluded that the pollution of nitrate at Fasarud Plain is in the desirable and moderate range.

Temporal trend analysis of nitrate

Values of normality using the Shapiro-Wilk test and consequent temporal trend using the Pearson method and the Spearman's Rho test for normal and non-normal values of nitrate, respectively, from April 2017 to March 2018 represented in Table 3.

Nitrate concentration in most wells followed the normal distribution except the Wells 18, 19, 22, and 26. Besides, the temporal trend of nitrate concentration in most wells was positive that means the nitrate concentration in most wells is ascending from April 2017 to March 2018. The highest enhancement of nitrate took place in Wells 1, 6, 9, 11, 13, 15, 16, 18, 26, and 28 at the significance level of 1%, and in the next rank in Wells 4, 20, 24, and 31 at the significance level of 5%. Besides, in Wells 8, 19, 21, and 29, the

Table 3 Normality and temporal trend tests of nitrate (from April 2017 to March 2018)

Well number	Longitude (E)	Latitude (N)	Normality		Trend
			Normal	Non-Normal	
1	54.493	28.726	0.633		0.827**
2	54.456	28.746	0.914		0.206
3	54.446	28.747	0.195		0.177
4	54.428	28.732	0.357		0.758*
5	54.339	28.726	0.131		0.548
6	54.397	28.736	0.975		0.808**
7	54.395	28.725	0.849		0.073
8	54.317	28.666	0.357		-0.214
9	54.334	28.662	0.797		0.949**
10	54.286	28.729	0.056		0.654
11	54.299	28.709	0.050		0.826**
12	54.266	28.742	0.934		0.552
13	54.246	28.793	0.097		0.843**
14	54.281	28.775	0.976		0.242
15	54.281	28.798	0.362		0.983**
16	54.504	28.753	0.158		0.901**
17	54.474	28.733	0.151		0.612
18	54.486	28.748		0.002**	0.983**
19	54.448	28.729		0.009**	-0.183
20	54.457	28.741	0.096		0.668*
21	54.462	28.750	0.659		-0.485
22	54.498	28.743		0.006**	0.433
23	54.491	28.746	0.122		0.156
24	54.424	28.759	0.698		0.795*
25	54.083	28.752	0.120		0.645
26	54.414	28.750		0.035*	0.867**
27	54.378	28.446	0.257		0.166
28	54.378	28.781	0.092		0.928**
29	54.323	28.784	0.524		-0.690*
30	54.370	28.788	0.050		0.043
31	54.372	28.787	0.903		0.670*

*Statistically significant trends at the 5% significance level

**Statistically significant trends at the 1% significance level nitrate concentration trend was descending that only Well 29 had a significant decrease at the significance level of 1%.

The Wells had the increasing temporal trend of nitrate, are on the way of groundwater dominant flow or have the formations of Gurpi, Asmari, or Tarbur. Besides, well 29 with the significant decreasing trend of nitrate at 1% level is in the vicinity of salt diapir of Korsia. These results show that the reason for nitrate changes from April 2017 to March 2018 cannot be geological formations. Therefore, the agricultural drainage can be the main reason for nitrate increasing trend in the studied wells. Liu et al. (2017) resulted that the temporal variability of groundwater nitrate in Shandong Province, China, had a certain trend over the years. Mohammadi et al. (2017) based on the zoning maps of groundwater in Bandar-e Gaz City, Iran, found that in the dry seasons, nitrate and hardness concentration is more than rainy seasonal.

Spatial trend analysis of nitrate

Nitrate concentrations ranged between 2.43 and 96 mg L^{-1}. The most values that characterize the waters of the western, eastern, southern, and north-western areas of the aquifer relate to the groundwater flow direction and fertilization of agricultural lands. The spatial distribution of NO_3 concentration is represented in Fig. 2. Nitrate is a very essential factor for evaluating the contamination of groundwater resources. This parameter is related to the desirable limit of 50 mg L^{-1} in 194 samples (70%). No water sample is within the maximum permissible limit. In the survey region, 85 water samples (30%) exceed the nitrate concentration limit (50 mg L^{-1}).

The results of normality test using the Shapiro-Wilk method and consequent spatial trend using the Pearson method and the Spearman's Rho test for normal and non-normal values of area percentage of nitrate classes, respectively, from April 2017 to March 2018 represented in Table 4. According to results, the area percentage of classes 1 (desirable limit) and 3 (not permissible limit) followed the normal distribution at the significance level of 5% and class 2 (maximum permissible limit) did not have any records throughout the plain.

Also, the spatial trend of area percentage of nitrate classes was negative and positive for classes 1 and 3, respectively. These results mean that from April 2017 to March 2018, the area percentage of class 1 (in desirable range) is descending and conversely the area percentage of class 3 (in not permissible range) is increasing. In general, the spatial trend of nitrate concentration in Fasarud Plain groundwater deteriorated from April 2017 to March 2018. Liu et al. (2017) showed that the spatial semivariogram can be impressed by intrinsic (physical, chemical, and biological characteristics of hydraulic and geographic conditions) and/or extrinsic (agricultural management practices, such as fertilization, irrigation, and animal wastes) parameters.

The NPI ranged between 0.88 and 3.8. According to the spatial distribution of NPI shown in Fig. 3, the lowest values of NPI related to clean water in terms of anthropogenic nitrate are observed in areas around the Wells 10, 24, 32, and 33. The light nitrate pollution based on NPI values is dominant over the most area especially from north to south of central areas during the most studied period. The NPI values demonstrated the anthropogenic nitrate pollution at moderate, significant, and very significant levels are most common in the northwest and eastern regions that vary over the irrigation season. That way, these areas are reduced from April 2017 to July 2017 due to diminishing the irrigation practices, but beginning the irrigation period from August or September 2017 causes to increase these classes of NPI.

According to the NPI and the nitrate concentration, wells were categorized into five classifications (lower than 20 mg L^{-1}, 20–40 mg L^{-1}, 40–60 mg L^{-1}, 60–80 mg L^{-1}, and more than 80 mg L^{-1}). About 24% of the samples had a nitrate concentration that lowered the threshold amount of the anthropogenic source or the human-affected amount (20 mg L^{-1}). About 30% of the sampled sites had a nitrate concentration of greater than 20 mg L^{-1} and less than 40 mg L^{-1} (light pollution), while 19% of the sampled sites had a nitrate concentration of greater than 40 mg L^{-1} and less than 60 mg L^{-1} (moderate pollution), 16% of sampled sites had a nitrate concentration of greater than 60 mg L^{-1} and less than 80 mg L^{-1} (significant pollution), and 11% of samples had a nitrate concentration of greater than 80 mg L^{-1} (very significant pollution).

Based on similar studies in other parts of the country in recent years, it was recognized that nitrate had an increasing trend, like in the study of temporal and spatial variations of drinking water sources of

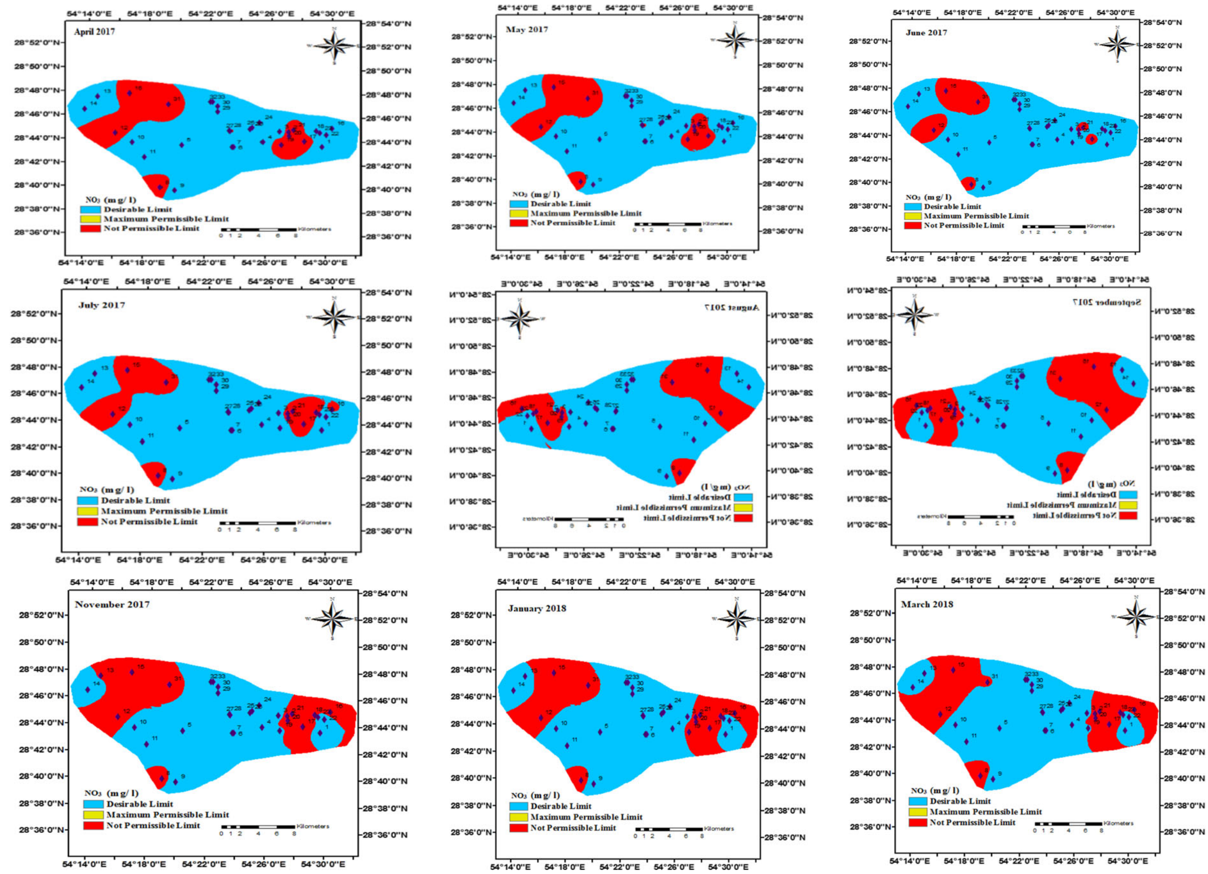

Fig. 2 Spatial distribution map of nitrate (from April 2017 to March 2018)

Table 4 Normality and spatial trend tests of area percentage of nitrate classes

Class	Normality		Trend
	Normal	Non- Normal	
1	0.2*		− 0.732*
2	–	–	–
3	0.2*		0.722*

*Statistically significant trends at the 5% significance level

**Statistically significant trends at the 1% significance level

Gachsaran, Iran, using GIS (Yousefi et al. 2013). Mozafarizadeh and Sajadi (2014) investigated the chemical pollution of Borazjan's groundwater, Iran, and presented high nitrate pollution up to 160 ppm, especially in the southern Borazjan plains which were occurred by farming activity and absorbing wells.

But Almasi et al. (2016) resulted that there was not a serious problem with nitrate and nitrite concentrations in groundwater of Dehloran and pollutant levels were less than standards. The soils in Dehloran are well-drained, so they have a low capacity to hold water; hence, these soils require some of the highest utilization of fertilizer and irrigation. The results of the current research are in agreement with Alighardashi and Mehrani (2017), who concluded that water use in agricultural areas and the subsequent consumption of fertilizer are the main sources of groundwater contamination with nitrate in Iran. Esmaeili et al. (2014) indicated that nitrate leaching is especially important in regions of intensive farming of Isfahan suburb, but municipal sewage effluents and industrial wastewaters are further sources of nitrate pollution in the adjacent of urban and industrial croplands. They concluded that the nitrate amount of groundwater in the survey area has considerably enhanced because of arid and semi-arid climatic conditions, the indiscriminate

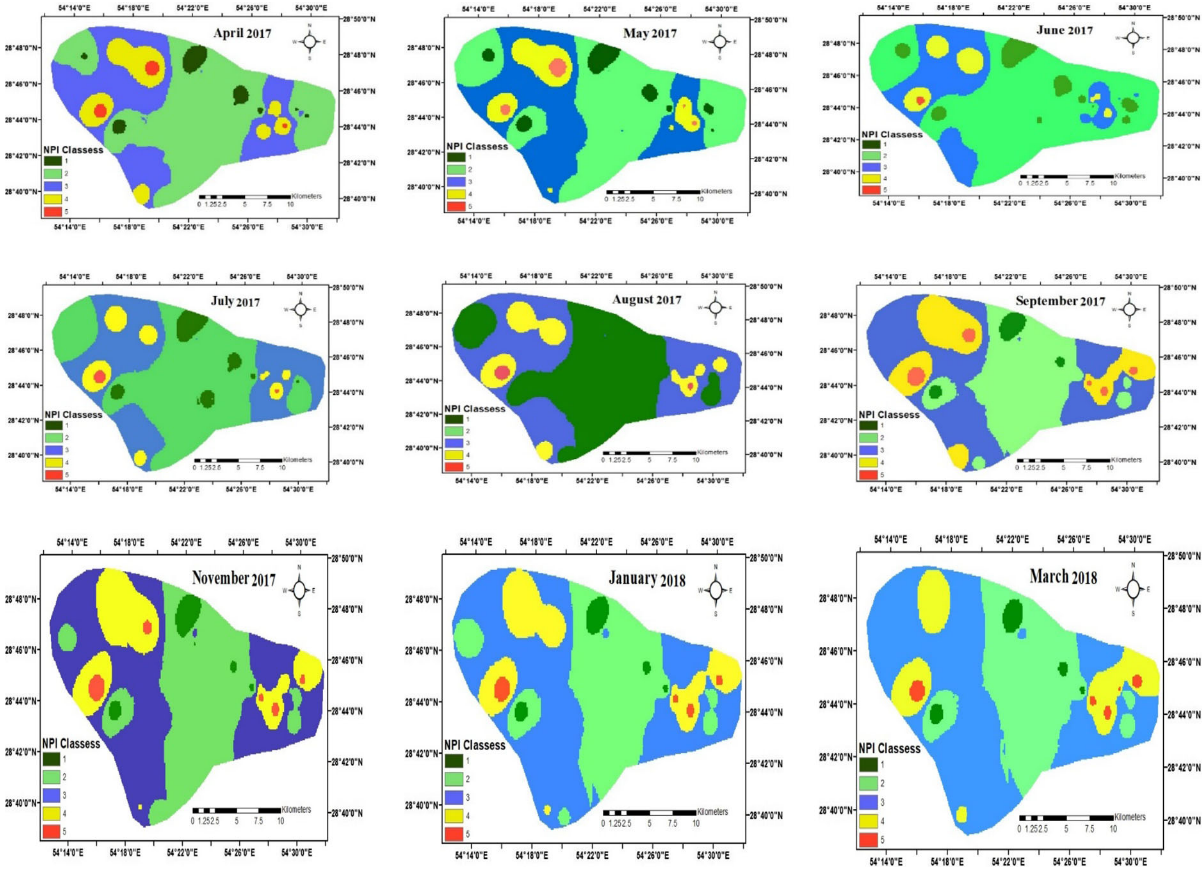

Fig. 3 Spatial distribution map of NPI (from April 2017 to March 2018)

exploitation of groundwater, recent droughts, high usage of fertilizers, and enhance of urbanization and industrialization.

Liu et al. (2017) proved that the significant variables for nitrate variance are livestock per unit area, annual mean temperature, vegetable yield per unit area, percentages of irrigation areas, population per unit area, percentages of orchard area, per capita agricultural production, and unit-area nitrogen fertilizer. Generally, statistical analysis indicated that there are many impressing parameters for nitrate variation in space and time (Liu et al. 2017). Deficit irrigation has been suggested as an alternative to decrease nitrate leaching (Amiri et al. 2016). On the other hand, using high nitrate water resources for irrigation can decrease the requirement for inorganic fertilizers and decrease the cultivation cost and nitrate contamination (Esmaeili et al. 2014).

Conclusion

Assessing the temporal and spatial trend of nitrate contamination and nitrate pollution index (NPI) in Fasarud Plain groundwater, southern Iran from April 2017 to March 2018 indicated that increasing temporal trend of nitrate is because of fertilizers using in agricultural lands. As, in most wells, the nitrate concentration and the NPI were increased temporally.

The spatial trend of area percentage of nitrate class 1 (desirable limit of less than 50 mg L^{-1}) was decreasing during the studied period, while its own for class 3 (not permissible limit of more than 50 mg L^{-1}) was increased. In general, results demonstrated that by finishing the irrigation season (about April 2017), nitrate concentration and the NPI reduced temporally in the samples and the percentage area of nitrate class 3 decreased gradually. Beginning the agricultural season (about September 2017), again the NPI, the nitrate concentration, and the percentage area of nitrate class 3 began to increase. Temporal and spatial variations of NPI are corroborated of anthropogenic nitrate pollution in the northwest, eastern, and south of the plain that vary over the irrigation season. As regards groundwater in this plain is also used for drinking purposes, the results of this study can be a warning to water resources authorities and decision makers.

Acknowledgements The authors would like to thank water laboratories of Fasa University and Darab University for providing the facilities to perform this research.

References

Abou Zaki, N., Torabi Haghighi, A., Rossi, P. M., Tourian, M. J., & Kløve, B. (2019). Monitoring groundwater storage depletion using Gravity Recovery and Climate Experiment (GRACE) data in Bakhtegan Catchment Iran. *Water, 11*(7), 1–13.

Akale, A. T., Moges, M. A., Dagnew, D. C., Tilahun, S. A., & Steenhuis, T. S. (2018). Assessment of nitrate in wells and springs in the North Central Ethiopian Highlands. *Water, 10*, 476. https://doi.org/10.3390/w10040476.

Akhavan, S., Zare Abyaneh, H., & Bayat Varkeshi, M. (2014). A systematic review on nitrate concentration in water resources of Iran. *Iranian Journal of Health & Environment, 7*(2), 205–228.

Alighardashi, A., & Mehrani, M. J. (2017). Survey and zoning of nitrate-contaminated groundwater in Iran. *Journal of Materials and Environmental Sciences, 8*(10), 2785–2794.

Almasi, A., Shokri, R., Momenzadeh, R., Rezaei, S., Jamshidi, A., & Yazdizadeh, R. (2016). Distribution of groundwater nitrate in Dehloran, Iran: A case study using GIS. *Journal of Advances in Environmental Health Research, 4*(3), 155–160.

Ameur, M., Hamzaoui-Azaza, F., & Gueddari, M. (2016). Nitrate contamination of Sminja aquifer groundwater in Zaghouan, northeast Tunisia: WQI and GIS assessments. *Desalination and Water Treatment*. https://doi.org/10.1080/19443994.2015.1137495.

Amiri, M. J., Hamidifar, H., Bahrami, M., & Eslamian, S. (2016). Optimisation of deficit-irrigation under variable seasonal rainfall and planning scenarios for rice in a semi-arid region of Iran. *International Journal of Hydrology Science and Technology, 6*(4), 331–343.

APH Association. (1998). *Standard methods for the examination of water and waste water*, 21st ed. Washington, DC: American Public Health Association.

Akpan, A. E., Ugbaja, A. N., Okoyeh, E. I., & George, N. J. (2018). Assessment of spatial distribution of contaminants and their levels in soil and water resources of Calabar, Nigeria using geophysical and geological data. *Environmental Earth Sciences, 77*(1), 13.

Badee Nezhad, A., Emamjomeh, M. M., Farzadkia, M., Jonidi Jafari, A., Sayadi, M., & Davoudian Talab, A. H. (2017). Nitrite and nitrate concentrations in the drinking groundwater of Shiraz City, South-central Iran by statistical models. *Iranian Journal of Public Health, 46*(9), 1275–1284.

Bahrami, M., Bazrkar, S., & Zarei, A. R. (2018). Modeling, prediction and trend assessment of drought in Iran using standardized precipitation index. *Journal of Water and Climate Change*. https://doi.org/10.2166/wcc.2018.174.

Bahrami, M., Zarei, A. R., & Chakav, S. (2017). Analysis of drought transitions using log-linear models in Iran. *International Journal of Water, 11*(3), 266–278.

Beiranvand, B., Ghasemi-Nejad, E., Kamali, M. R., & Ahmadi, A. (2014). Sequence stratigraphy of the Late Cretaceous-Paleocene Gurpi Formation in southwest Iran. *GeoArabia, 19*(2), 89–102.

Chand, S., Ashif, M., Zargar, M. Y., & Ayub, B. M. (2011). Nitrate pollution: a menace to human, soil, water and plant. *Universal Journal of Environmental Research and Technology, 1*, 22–32.

Devendra, P., Yashwant, B. K., Pradeep, P. K., & Vilas, R. C. (2016). Nitrate contamination indexing of subsurface water of upper Wainganga Drainage Basin of India. *International Journal of Innovative Research in Science, Engineering and Technology, 5*(1), 161–170.

Ducci, D., Della Morte, R., Mottola, A., Onorati, G., & Pugliano, G. (2019). Nitrate trends in groundwater of the Campania region (southern Italy). *Environmental Science and Pollution Research, 26*(3), 2120–2131.

Ducci, D. (2018). An easy-to-use method for assessing nitrate contamination susceptibility in groundwater. *Geofluids*. https://doi.org/10.1155/2018/1371825.

Esmaeili, A., Moore, F., & Keshavarzi, B. (2014). Nitrate contamination in irrigation groundwater, Isfahan, Iran. *Environmental Earth Sciences*. https://doi.org/10.1007/s12665-014-3159-z.

Fienen, M. N., & Arshad, M. (2016). The international scale of the groundwater issue. In A. J. Jakeman, O. Barreteau, R. J. Hunt, J. D. Rinaudo, & A. Ross (Eds.), *Integrated groundwater*. Cham: Springer.

Green, C. T., Liao, L., Nolan, B. T., Juckem, P. F., Shope, C. L., Tesoriero, A. J., et al. (2018). Regional variability of nitrate fluxes in the unsaturated zone and groundwater, Wisconsin, USA. *Water Resources Research, 54*(1), 301–322.

Guangwei, H. (2013). Characterization of nitrate contamination in an arid region of China. *Journal of Environmental Protection, 4*, 46–52.

Han, L., Huang, M., Ma, M., Wei, J., Hu, W., & Chouhan, S. (2018). Evaluating sources and processing of nonpoint source nitrate in a small suburban watershed in China. *Journal of Hydrology, 559*, 661–668.

Hoseinzadeh, E., Wei, C., Chavoshi, E., & Faghih, M. A. (2016). Groundwater quality and nitrate pollution modeling: an integrated study of contour mapping and geographic information system. *Desalination and Water Treatment*. https://doi.org/10.1080/19443994.2016.1150886.

Institute of Standard and Industrial Research of Iran (ISIRI). 2009. Standard number 1053: *Drinking water, physical and chemical characteristics* [in Persian].

Jahangeer Gupta, P. K., & Yadav, B. K. (2018). *Spatial and temporal nitrate transport in deep heterogeneous vadose zone of India's Alluvial Plain*. In V. Singh, S. Yadav, & R.

Yadava (Eds.), Groundwater. Water Science and Technology Library, Vol. 76. Singapore: Springer.

Liu, J., Jiang, L. H., Zhang, C. J., Li, P., & Zhao, T. K. (2017). Nitrate-nitrogen contamination in groundwater: Spatiotemporal variation and driving factors under cropland in Shandong Province, China. In *IOP conference series: Earth and environmental science*, 82.012059

Maghanga, J. K., Kituyi, J. L., Kisinyo, P. O., & Ng'etich, W. K. (2013). Impact of nitrogen fertilizer applications on surface water nitrate levels within a Kenyan Tea Plantation. *Journal of Chemistry*, 196516.

Maghfouri-Moghadam, I., Zarei-Sahamieh, R., Ahmadi-Khalaji, A., & Tahmasbi, Z. (2009). Microbiostratigraphy of the Tarbur Formation, Zagros Basin, Iran. . *Journal of Applied Sciences, 9*, 1781–1785.

Maghfouri Moghaddam, R., & Khanjai, Z. (2014). Microbiostratigraphy of the Oligo- Miocene Asmari Formation, Kuh Siah Anticline (Izeh Basin), SW Iran. *Iranian Journal of Earth Sciences, 6*, 114–120.

Michel, D., Pandya, A., Hasnain, S. I., Sticklor, R., & Panuganti, S. (2012). *Water challenges and cooperative response in the Middle East and North Africa*. New York: Brookings Institution. Available at https://www.brookings.edu/about/projects/islamic-world.

Mir, S. A., Qadri, H., Beigh, B. A., Dar, Z. A., & Bashir, I. (2019). Assessment of nutrient status and water quality index of Rambiara stream, Kashmir Himalaya, India. . *Journal of Pharmacognosy and Phytochemistry, 8*(3), 172–180.

Mohammadi, A. A., Yaghmaeian, K., Faraji, H., Nabizadeh, R., Dehghani, M. H., Khail Khaili, J., et al. (2017). Temporal and spatial variation of chemical parameter concentration in drinking water resources of Bandar-e Gaz City using Geographic Information System. *Desalination and Water Treatment, 68*, 170–176.

Mojid, M. A., Parvez, M. F., Mainuddin, M., & Hodgson, G. (2019). Water table trend—A sustainability status of groundwater development in North-West Bangladesh. *Water, 11*, 1182.

Mokarram, M., Hamzeh, S., Aminzadeh, F., & Zarei, A. R. (2015a). Using machine learning for land suitability classification. *West African Journal of Applied Ecology, 23*(1), 63–73.

Mokarram, M., Mmahmoodi, A. R., & Zarei, A. R. (2015b). Using geostatistic analysis for prediction of SAR in south of Iran. *Journal of Industrial Pollution Control, 31*(2), 143–148.

Mokarram, M., Mokarram, M. J., Zarei, A. R., & Safari Nejadian, B. (2015c). The use of adaptive neuro-fuzzy network (ANFIS) to predict water quality. *Journal of Ecohydrology, 4*(2), 547–557. **(In Persian)**.

Mousavi, S. F., & Amiri, M. J. (2012). Modelling nitrate concentration of groundwater using adaptive Neural-Based Fuzzy Inference System. *Soil and Water Research, 7*(2), 73–83.

Mozafarizadeh, J., & Sajadi, Z. (2014). Survey of groundwater chemical pollution in the Borazjan plain. *Iranian South Medical Journal, 17*(5), 927–937. **(in Persian)**.

Mukherjee, A., Soumendra Nath, B., & Wada, Y. (2018). Groundwater depletion causing reduction of baseflow triggering Ganges river summer drying. *Scientific Reports, 8*, 12049.

Naseri, H., Raghimi, M., & Yakhkeshi, M. E. (2006). Investigation of the effective factors variation of nitrate concentration in the groundwater of Ghareso Watershed Basin Golestan Province. *Agricultural Science Nature, 13*(1), 1–9.

Nazaripour, H., Dostkamiyan, M., & Alizadeh, S. (2015). The spatial distribution patterns of temperature, precipitation, and humidity using geostatistical exploratory analysis (case study: Central Area of Iran). *Journal of the Earth and Space Physics, 41*(1), 99–101.

Nosrati, K., & Zareiee, A. R. (2011). Assessment of meteorological drought using SPI in West Azarbaijan Province, Iran. . *Journal of Applied Sciences and Environmental Management, 15*(4), 563–569.

Obeidat, M. M., Al-Ajlouni, A., Al-Rub, F. A., & Awawdeh, M. (2012). *An innovative nitrate pollution index and multivariate statistical investigations of groundwater chemical quality of Umm Rijam Aquifer (B4)*. North Yarmouk River Basin: INTECH Open Access Publisher, Jordan.

Ogrinc, N., Tamše, S., Zavadlav, S., Vrzel, J., & Jin, L. (2019). Evaluation of geochemical processes and nitrate pollution sources at the Ljubljansko polje aquifer (Slovenia): A stable isotope perspective. *Science of the Total Environment, 646*, 1588–1600.

Rawat, K. S., Jeyakumar, L., Singh, S. K., & Tripathi, V. K. (2019). Appraisal of groundwater with special reference to nitrate using statistical index approach. *Groundwater for Sustainable Development, 8*, 49–58.

Schipper, L. A., & Vojvodić-Vuković, M. (2000). Nitrate removal from groundwater and denitrification rates in a porous treatment wall amended with sawdust. *Ecological Engineering, 14*(3), 269–278.

Sneyers, R. (1990). *On the statistical analysis of series of observations*. World Meteorological Organization, Technical Note No. 143, WMO No. 415.

Sun, J., Li, Z., Xue, L., Wang, T., Wang, X., Gao, J., et al. (2018). Summertime C1–C5 alkyl nitrates over Beijing, northern China: spatial distribution, regional transport, and formation mechanisms. *Atmospheric Research, 204*, 102–109.

Turner, S. W. D., Hejazi, M., Yonkofski, C., Kim, S. H., & Kyle, P. (2019). Influence of groundwater extraction costs and resource depletion limits on simulated global nonrenewable water withdrawals over the twenty-first century. *Earth's Future, 7*, 123–135.

Voss, K. A., Famiglietti, J. S., Lo, M., Linage, C., Rodell, M., & Swenson, S. C. (2013). Groundwater depletion in the Middle East from GRACE with implications for transboundary water management in the Tigris-Euphrates-Western Iran region. *Water Resources Research, 49*(2), 904–914.

Wang, G. F., Satake, M., & Horita, K. (1998). Spectrophotometric determination of nitrate and nitrite in water and some fruit samples using column preconcentration. *Talanta, 46*, 671–678.

Water Health Organization (WHO). (2011). *Guidelines for drinking-water quality*, 4th edn. ISBN 9789241548151564.

Werner, A. D., Zhang, Q., Xue, L., Smerdon, B. D., Li, X., Zhu, X., et al. (2013). An initial inventory and indexation of groundwater mega-depletion cases. *Water Resour Manag, 27*(2), 507–533.

Yin, S., Xiao, Y., Gu, X., Hao, Q., Liu, H., Hao, Z., et al. (2019). Geostatistical analysis of hydrochemical variations and nitrate pollution causes of groundwater in an alluvial fan plain. *Acta Geophysica*, 1–13.

Yousefi, Z., Barafrashteh Pour, M., Taghavi, M., Mashayekh Salehi, A., & Sedaghat, F. (2013). Survey on temporal and spatial variation of nitrate and nitrite in drinking water of Gachsaran by using Geographic Information System (GIS). *Journal of Mazandaran University of Medical Sciences, 22*(2), 158–162. **(in Persian)**.

Zarei, A. R., & Bahrami, M. (2016). Evaluation of quality and quantity changes of underground water in Fasa plain, Fars (2006–2013). *Irrigation and Water Engineering Journal, 24*, 103–113. **(in Persian)**.